

Induced Super-halogen Behavior of Metal Moieties in Halogen-Doped Clusters: $\text{Li}_n\text{I}^{(-)}$ and $\text{Al}_n\text{I}^{(-)}$, $n = 13, 1, 2, 3$

Hobart Leung and Fedor Y. Naumkin*

Faculty of Science, University of Ontario Institute of Technology, Oshawa, Ontario L1H 7K4, Canada

Received: May 24, 2006; In Final Form: October 6, 2006

A comparative density functional theory (DFT) study of a series of neutral and negative-ionic lithium and aluminum clusters doped with iodine atom is presented. The I atom is found to preserve the same position at Li_{13} with and without the negative charge and Li_{13} to vary its shape from prolate to oblate with changing spin state of Li_{13}I . Both the Mulliken and natural charges are considered, the natural-charge separation between the metal and halogen moieties being generally much larger (except for Al_{13}I^-). In Li_nI^- , the additional electron is strongly localized on the metal moiety starting from $n = 1$, even though the electron affinity of Li_n is much smaller than that of I. Such a super-halogen behavior of Li_n is induced by highly electronegative iodine making the two components charged in Li_nI and leading to a charge–dipole interaction with the additional electron. In Al_nI^- , similar factors result in Al_n being more negative than I already for $n = 3$, even though the electron affinity of I is higher, the effect escalating for $n = 13$.

Introduction

Metal clusters have been intensely studied as intermediates between the individual atoms and bulk metals, in order to track the evolution of properties with an increasing amount of matter. Since the clusters have exhibited a unique behavior, such as nonmetallic character when being sufficiently small, or increased stability and extrema in other parameters (ionization potentials, electron affinities, etc.) at specific (“magic”) sizes, they have become objects of interest by themselves.¹ Their modern areas of application include new materials, catalysis, molecular electronics/photonics, and others.

Among the unusual properties of some metal clusters is a high electron affinity (EA) comparable to or even exceeding that of halogen atoms, as found, for instance, for Al_{13} ² and attributed to the closed electronic shell (with 40 valence electrons) of the cluster negative ion, Al_{13}^- . The neutral Al_{13} cluster has therefore been named “super-halogen” and proposed as a potential building unit for new materials. For instance, it might be incorporated as a cluster analogue of an electronegative atom in an ionic crystal. Other examples include, in particular, pure and doped gold clusters such as Au_{13} ³ and MAu_{12} ($M = \text{V}, \text{Nb}, \text{Ta}$)⁴. Earlier notions of super-halogens include theoretical predictions for Groups I–V atom super-halides,⁵ verified experimentally for the Group I and II cases.^{6,7}

The EA value of Al_{13} higher than that of I has also been referred to in interpreting the charge distribution in Al_{13}I^- , with the negative charge located mainly on the metal moiety.⁸ Moreover, the charge in Al_{13}I^- , according to the HOMO density, concentrates on the Al atom remotest from I. The latter feature, however, would not seem to follow from the relative EA values of the two components, but would rather fit the dipole field of the neutral metal–halogen system interacting with the additional electron.

The aim of this work is to investigate the origins of the above charge distribution and to try to understand what other factors

may be responsible for its features, in addition to the relative EA values of the constituent metal-cluster and halogen atom in the metal–halide cluster ions. For this purpose, one could consider another metal cluster, with EA lower relative to the halogen’s, and compare its behavior in a halide compound similar to that of Al_{13} . Alkali metals are ultimate “non-halogens”, so, for instance, Li_{13} is a reasonable candidate, whose similar closed-shell atomic but different open-shell electronic structure would make the comparison adequate. Besides, the Li_{13}I system has 20 valence electrons and is therefore also interesting as a closed-shell species. Further, it is logical to look at smaller counterparts such as M_nI^- ($M = \text{Li}, \text{Al}; n = 1, 2, 3$) in order to check how the charge-distribution features evolve with the cluster size, as small M_n are known to be no super-halogens. The results of these studies are presented below.

Computational Procedure

Present calculations have been performed with the NWChem ab initio package⁹ and pictures generated using the Molekel software.¹⁰ For a consistent comparison with previous work,⁸ density functional theory (DFT) has been employed. The PBE0 functional, which showed a good performance for aluminum clusters,¹¹ was used. The cc-pVDZ basis set for Li and Al atoms and the LANL2DZ effective core potential plus corresponding basis set for the I atom (incorporated into NWChem) have been used. Neutral and ionic system geometries have been optimized for the low-energy electronic states with a few spin multiplicities. The optimization has involved all atoms and been done in the C_1 symmetry group in order to avoid additional geometry constraints able to lead to incorrect predictions of stable geometries.

Results of test calculations at this level of theory are compared in Table 1 with experimental data taken from a National Institute of Standards and Technology (NIST) online database.¹² As can be seen, the comparison is favorable for relevant atomic as well as diatomic species, the deviations not exceeding 3% in both characteristic energies and distances, except for D_e of metal

* To whom correspondence should be addressed. E-mail: fedor.naumkin@uoit.ca.

TABLE 1: Comparison of Calculated and Experimental Atomic and Diatomic Parameters

system	calculation	experiment ¹²
I	EA = 3.03 eV	3.06 eV
Li	IE = 5.57 eV	5.39 eV
LiI	$D_e = 3.66$ eV $R_e = 2.44$ Å	3.56 eV ^a 2.39 Å
Li ₂	$D_e = 0.83$ eV $R_e = 2.74$ Å	1.07 eV ^a 2.67 Å
Al	IE = 6.10 eV	5.99 eV
AlI	$D_e = 3.80$ eV $R_e = 2.59$ Å	3.84 eV ^a 2.54 Å
Al ₂	$D_e = 1.45$ eV $R_e = 2.49$ Å	1.63 eV ^a 2.47 Å

$${}^a D_e \approx D_0 + h\omega_e/2.$$

diatoms, underestimated by 10–20%. The latter deviation is, however, not crucial for this work.

Results and Discussion

Li₁₃I. The Li₁₃ cluster has previously been found (see, for instance, ref 10) to adopt icosahedral geometry in its ground state, similar to the Al₁₃ cluster. When the I atom is attached, its most stable position is predicted to be at the hollow site, above the center of the triangular unit of Li₁₃ (Figure 1a), unlike the bridging position between two surface atoms of Al₁₃.⁸ It should be noted here that later studies¹⁴ have found a low-symmetry structure of Al₁₃I to be lower in energy by ≈ 0.2 eV. However, it corresponds to a non-icosahedral shape of the Al₁₃ moiety, while it is interesting to make a comparison of systems with the metal components similar in shape. In this work we will therefore consider the above (bridge) low-energy isomer of Al₁₃I which (approximately) preserves the icosahedral Al₁₃ moiety. Its difference in the I position from Li₁₃I can be related to the directional character of the valence p-orbital of Al as compared to the isotropic s-orbital of Li, affecting the overlap with the p-orbital of I.

The lowest-energy state of Li₁₃I is predicted to be triplet, followed by quintet only 0.08 eV higher, while singlet is 0.52 eV above the (triplet) ground state. This is to be correlated with the Li₁₃ sextet ground state and the quartet state ≈ 1.2 eV above. The ground-state I-nearest Li distances in Li₁₃I are calculated to be ≈ 0.3 Å longer relative to that in the LiI diatom (Table 2), which could be expected in terms of a reduced overlap of the Li s-orbital and I p-orbital (not pointing directly to Li). The Li₁₃ moiety is slightly elongated in the direction to iodine, with the distances between the opposite Li atoms (through the center of the cluster) being 6.0 ± 0.1 Å, which is ≈ 0.2 Å longer than for such distances in the (approximately) perpendicular direction. The energy for detaching the iodine is found to be ≈ 0.4 eV larger compared to that for LiI (Table 2), apparently as a result of interaction with more than one lithium (at least three nearest).

It is interesting that, for the singlet state, the Li₁₃ moiety is somewhat compressed along the direction to I, as is visible in Figure 1b, with the through-center Li–Li distances of 5.69 Å, significantly shorter (by 0.54 Å) than in the perpendicular direction. The quintet state, in turn, corresponds to the Li₁₃ moiety more spherical, with the distances between the opposite Li atoms within 5.9 ± 0.1 Å. The I-nearest Li distances are almost unchanged from the ground state, at 2.76 ± 0.03 Å for both singlet and quintet.

Charge distributions have been evaluated in terms of both the Mulliken and the natural charges on atoms (from the natural atomic and bond orbital analysis), the latter values being presented hereafter by default. The results for the ground state

are collected in Table 3 and indicate a negative charge on the I atom, as expected, from both approaches, the Mulliken value being much smaller.

It should be noted that at present the natural-charge values are commonly considered as more reliable since they are much less sensitive to the basis set. Another, more specific reason relevant to this work is the unreasonably high Mulliken charges on the internal atoms of metal clusters, for instance central atoms of icosahedral 13-atom systems.¹⁵ In particular for the present case of Li₁₃I, the (positive) Mulliken charge on Li_{central} of the Li₁₃ moiety is found to exceed the Li-nucleus charge. On the other hand, the natural charge on Li_{central} is negative (-0.65 e). Similar method-related features of the charge distribution are obtained for isolated Li₁₃ as well (with the natural charge of -0.52 e on Li_{central}). Such a concentration of the electron density in the center of a metal cluster seems to be rather counterintuitive, even taking into account the cluster's possible nonmetallic character at such a small scale.

In terms of the natural charges, three Li atoms nearest to I and thus between the two negative centers carry most of the positive charge, $+0.93$ e (Figure 1a), followed by a ring of six peripheral Li atoms less positive and then by three lithiums (most remote from I) still more weakly charged. The Li₁₃ moiety in Li₁₃I is thus strongly polarized due to I. Interestingly, the higher-energy singlet state exhibits a layered alternate-sign charge distribution (Figure 1b) with the charge on the 3-Li unit near I reaching $+1.45$ e, followed by a negatively charged 6-atom ring at -0.78 e around the central atom (with -0.58 e), and then by the 3-Li unit most remote from I with $+0.67$ e charge. The corresponding Mulliken distribution, on the other hand, shows the near-I three lithiums most negative and no charge-layers instead.

In the present work, of main concern is the charge separation between the iodine and lithium moieties. Such a property is directly related to the system dipole moment. Its ab initio value is ≈ 2.8 D (for either the ground or the singlet state), and the direction is in accord with the positively charged metal moiety.

Li₁₃I⁻. When another electron is added to Li₁₃I, the lowest-energy structure still has iodine at the hollow site (Figure 1c), compared to the (changed) position on top of a single metal atom in Al₁₃I⁻.⁸ This can be looked at, in a simplistic way, as I⁻ sphere (in terms of unperturbed electron density) lying comfortably between three other Li spheres. The ground state is predicted to be sextet, with the quartet and doublet only 0.075 and 0.12 eV above. The ground-state I-nearest Li distances slightly stretch (within 0.1 Å, Table 2) relative to the neutral counterpart, consistent with increasing internuclear distance in LiI⁻ relative to LiI, and is essentially invariant (within 0.01 Å) for quartet and doublet. The Li₁₃ moiety is almost symmetric for all spin states, with only minor compression or elongation in the direction to I (within 0.1 Å) and is essentially of the same size (about 5.9 Å in diameter) as in the neutral system. The binding energy of I⁻ to Li₁₃ is ≈ 1.1 eV larger than for LiI⁻, and ≈ 1.6 eV smaller than for Li₁₃I (Table 2), similar to its reduction for LiI⁻ relative to LiI. For both the neutral and ionic clusters, this binding energy is relative to the lowest-energy sextet state of Li₁₃.

The electron affinity of Li₁₃I is predicted to be 1.47 eV, intermediate between ≈ 3 eV for I and 0.92 eV of Li₁₃ (with the latter obtained relative to the lowest-energy quintet state of Li₁₃⁻). This indicates that the additional electron in Li₁₃I⁻ is significantly delocalized between the metal cluster and iodine.

Indeed, the charge on I increases only slightly in Li₁₃I⁻ relative to Li₁₃I (Table 3), according to both the Mulliken and

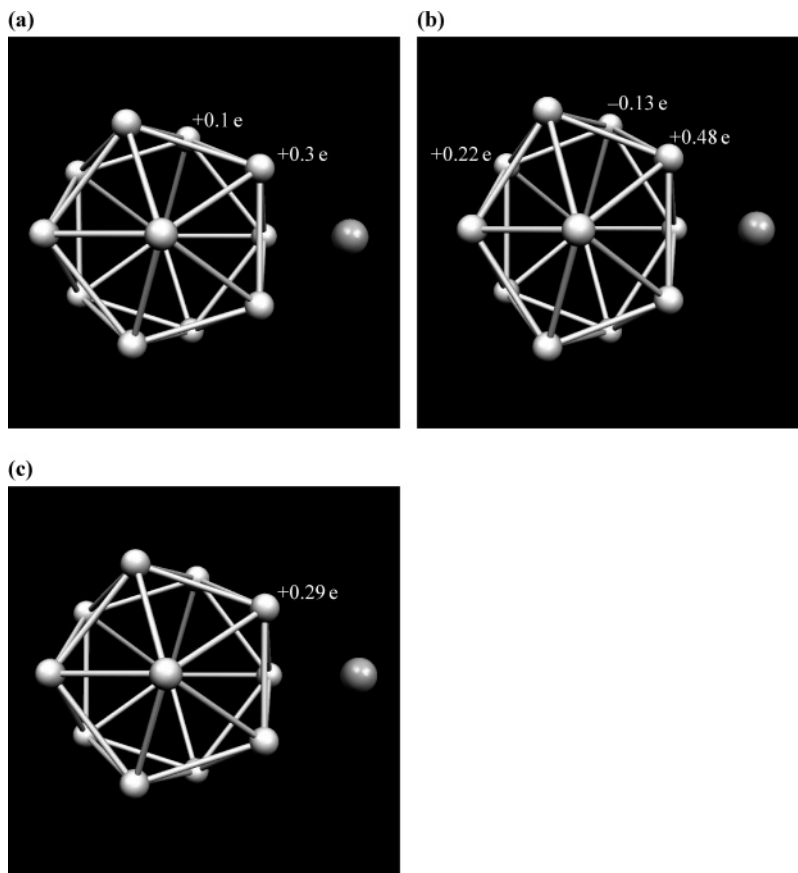


Figure 1. Optimized geometries and atomic natural charges of Li_{13}I (a) triplet and (b) singlet and (c) Li_{13}I^- sextet.

TABLE 2: Calculated Equilibrium Parameters of the Ground-State Systems

system, $M_n\text{I}^{(-)}$	$D_e(M_n\text{I}^{(-)})/\text{eV}$	$R_e(M\text{I})/\text{\AA}$
Li_{13}I	4.08	2.73–2.76
Li_{13}I^-	2.51	2.80
Li_2I (T-shaped)	3.84	2.63
Li_2I^- (T-shaped)	1.44	2.69
Al_2I (T-shaped)	3.56	2.86
Al_2I^- (T-shaped)	1.54	3.03
Al_3I	3.20	2.52
Al_3I^-	2.15	2.66
Al_{13}I	2.8	2.79–2.84
Al_{13}I^-	3.03, 2.49 ^a	2.58

^a $D_e(\text{I}:\text{Al}_{13}^-)$

natural values, so that most of the additional-electron charge (>90%) goes to the Li_{13} moiety, making it negatively charged. The negative charge already present on I in the neutral system thus largely *remains* on iodine in the ionic system, and the additional electron is attracted almost entirely to the positively charged lithium cluster within Li_{13}I , consistent with a simple electrostatic picture of the charge–dipole interaction. The EA value of Li_{13}I , much closer to that for Li_{13} than for I, also confirms that it is the metal moiety which accommodates the additional electron.

The natural charge on the central atom of the Li_{13} moiety increases to -0.92 e in Li_{13}I^- . In the isolated Li_{13}^- , by comparison, this charge is reduced (to -0.38 e) relative to the neutral cluster, so the presence of I has a substantial effect on the charge distribution. The three Li atoms nearest to I remain positively charged ($+0.86$ e altogether) in Li_{13}I^- , while the rest of the atoms are essentially neutral (Figure 1c).

It is worth emphasizing that the low and high EA values of isolated Li_{13} and I, respectively, are thus not the main factors

affecting the additional-electron preferred location on Li_{13} . This location is actually determined by the respectively high and low effective electron affinities of the metal and halogen moieties having ionic characters ($\text{Li}_{13}^{\delta+}$ and $\text{I}^{\delta-}$) inside Li_{13}I . The Li_{13} cluster, no super-halogen in terms of its EA value, therefore exhibits a super-halogen behavior (by winning the additional electron from I) within Li_{13}I , and this behavior is induced by iodine. The effect is even more dramatic in terms of the Mulliken charges showing that most of the negative charge in Li_{13}I^- is on Li_{13} (Table 3), with a similar result obtained previously for Al_{13} in Al_{13}I^- .⁸

Model. A simple model supporting the above considerations can be suggested as follows. Consider a partially charged species (within a system) as a formal combination of its purely neutral and purely ionic forms, with the ionic character determined by the (absolute) charge value; i.e., $A^{\delta\pm} \approx (1 - \delta)A + \delta A^\pm$. If we adopt the ionization energy IE of the neutral species as EA of the corresponding positive ion, then

$$\text{EA}(\text{Li}_{13}^{\delta+}) \approx (1 - \delta)\text{EA}(\text{Li}_{13}) + \delta\text{EA}(\text{Li}_{13}^+) = (1 - \delta)\text{EA}(\text{Li}_{13}) + \delta\text{IE}(\text{Li}_{13})$$

$$\text{EA}(\text{I}^{\delta-}) \approx (1 - \delta)\text{EA}(\text{I}) + \delta\text{EA}(\text{I}^-)$$

From the second equation it is clear that the higher the negative charge on the halogen moiety, the less electronegative it will be, as the Coulomb repulsion of the additional electron from the negative ion can even make its EA negative. Indeed, calculation at the same level of theory as before gives the energy of I^{2-} as 19.5 eV above that for I^- , so that we can put $\text{EA}(\text{I}^{2-}) \approx -19.5$ eV for our purpose. It is worth noting that we do not put $\text{EA}(\text{I}^-) = 0$, since this would omit the actually present repulsion of the additional electron from $\text{I}^{\delta-}$ in Li_{13}I . In other

TABLE 3: Charges (in e) on the Lithium and Iodine Moieties in the Ground-State Systems

method	Li _n I	Li _n I ⁻	difference (additional electron)
Mulliken	$q(\text{Li}_{13})/q(\text{I}) = \pm 0.09$	-0.82/-0.18	-0.91/-0.09
	$q(\text{Li})/q(\text{I}) = \pm 0.32$	-0.41/-0.59	-0.73/-0.27
	$q(\text{Li}_2)/q(\text{I}) = \pm 0.15$	-0.75/-0.25	-0.90/-0.10
natural	$q(\text{Li}_{13})/q(\text{I}) = \pm 0.77$	-0.20/-0.80	-0.97/-0.03
	$q(\text{Li})/q(\text{I}) = \pm 0.85$	-0.09/-0.91	-0.94/-0.06
	$q(\text{Li}_2)/q(\text{I}) = \pm 0.83$	-0.11/-0.89	-0.94/-0.06

TABLE 4: Charges (in e) on the Aluminum and Iodine Moieties in the Ground-State Systems

method	Al _n I	Al _n I ⁻	difference (additional electron)
Mulliken	$q(\text{Al}_{13})/q(\text{I}) = \pm 0.05$	-0.72/-0.28	-0.77/-0.23
	$q(\text{Al})/q(\text{I}) = \pm 0.21$	-0.44/-0.56	-0.65/-0.35
	$q(\text{Al}_2)/q(\text{I}) = \pm 0.17$	-0.44/-0.56	-0.61/-0.39
	$q(\text{Al}_3)/q(\text{I}) = \pm 0.14$	-0.61/-0.39	-0.75/-0.25
natural	$q(\text{Al}_{13})/q(\text{I}) = \pm 0.13$	-0.68/-0.32	-0.81/-0.19
	$q(\text{Al})/q(\text{I}) = \pm 0.55$	-0.29/-0.71	-0.84/-0.16
	$q(\text{Al}_2)/q(\text{I}) = \pm 0.49$	-0.43/-0.57	-0.92/-0.08
	$q(\text{Al}_3)/q(\text{I}) = \pm 0.30$	-0.54/-0.46	-0.84/-0.16

words, we should not conclude that electron will fly away from I⁻ as it likely would from isolated I⁻, since in the former case the electron is kept in the system by Li₁₃^{δ+}. Besides, the use of the limited basis set for I²⁻, lacking diffuse functions (hence effectively confining the electron close to the ion), is consistent, as it is this basis set which is used to describe the total system (Li₁₃I⁻) and its relevant component (I^{δ-}).

Taking the δ value from Table 3, we obtain EA(I^{δ-}) \approx 1.0 and -14 eV for the Mulliken and natural charges, respectively. Since EA(Li₁₃^{δ+}) is to be positive anyway, the natural-charge based result already implies the additional electron's strong preference of the metal moiety. The ionized Li₁₃⁺ cluster has been optimized at the same level of theory for a few spin states and the quintet found to be the ground state. The calculated IE(Li₁₃) = 4.85 eV in combination with the above-mentioned EA(Li₁₃) = 0.92 eV results in EA(Li₁₃^{δ+}) \approx 1.3 and 4.0 eV for the Mulliken and natural charges, respectively. As can be seen, the charges on the metal and halogen moieties within the cluster can indeed affect their electronegativities considerably.

It should be noted that in the earlier discussion EA of Li₁₃I has been compared to those of neutral rather than charged metal and halogen moieties. This, however, does not affect the conclusion: the value for the cluster is still much closer to EA-(Li₁₃^{δ+}) than to EA(I^{δ-}), for both Mulliken and natural charges. The reason is the larger difference between the EA values for the neutral iodine and for the charged iodine moiety, as a result of the much larger difference between EA(I) and EA(I⁻) than between EA(Li) and EA(Li⁺).

Besides, the EA(Li₁₃I) value remains between EA for Li₁₃^{δ+} and I^{δ-} because they are respectively larger and lower compared to those for Li₁₃ and I. Similar considerations apply also to other species below.

LiI and Li₂I. At this stage, it is interesting to check if similar features can be found for smaller counterparts such as LiI and Li₂I. For consistency, calculations for these species have been carried out at the same PBE0/cc-pVDZ (Li) + LANL2DZ (I) level of theory.

In LiI, the charge separation is stronger compared to Li₁₃I due to a lower electronegativity of Li, the variation being less significant for the natural charges (Table 3). When another electron is added and LiI⁻ formed, the negative charge on Li is smaller than that on Li₁₃ in Li₁₃I⁻, as a reflection of the lower EA value of Li. The negative charge on I increases only slightly in LiI⁻ relative to LiI (especially for the natural-charge case), so the additional electron is localized almost entirely at the Li

end of the molecule, similar to the Li₁₃I case. The Li atom, an ultimate non-halogen with a low EA value, still wins the additional electron from iodine and thus demonstrates a super-halogen behavior within LiI. This is due to the charge distribution in the neutral LiI (i.e., Li^{δ+}I^{δ-}), in analogy with the larger cluster. The Mulliken charges show the same effect, even though somewhat less strongly. According to the above model (section Li₁₃I), EA(I^{δ-}) is negative for both Mulliken and natural charges, supporting the preferred location of the additional electron.

The Li₂I case is intermediate between LiI and Li₁₃I in terms of charges (Table 3) as well as binding energies (Table 2). Here the optimized isosceles-triangular geometries of the Li₂I and Li₂I⁻ ground states are considered. The Mulliken charges in Li₂I approach those in Li₁₃I, while the natural-charge values are close to those in LiI. There is thus a trend in the variation of the system parameters with increasing size of the metal moiety, while its super-halogen behavior (in terms of the additional-electron localization) manifests itself at all sizes. The relative values of the negative charges on the metal moieties in Li_nI⁻ follow the relative EA values of Li_n, increasing from $n = 1$ to 2 to 13. The additional-electron localization on Li within LiI and on Li₂ within Li₂I is also reflected in their relatively low electron affinities (under 1 eV).

AlI and Al₂I. In the above sections it is shown that the super-halogen behavior becomes somewhat stronger with increasing lithium-moiety size in Li_nI. In order to compare with the case of another metal, here we consider small aluminum moieties (correlating to the real, "permanent" super-halogen, Al₁₃).

The charge separation between the metal and halogen moieties in the neutral systems decreases from AlI to Al₂I, similar to the lithium case. The separation is, however, smaller than in the corresponding Li_nI (Table 4), considerably for the natural and less significantly for the Mulliken charges. This is consistent with the higher ionization energies of Al_n.

In AlI⁻ and Al₂I⁻, the negative charge is concentrated on I, but considerably less so than for the lithium case. The negative (natural) charge on the metal moiety increases from AlI⁻ to Al₂I⁻, in accord with increasing EA and similar to the Li-based counterparts, and approaches a near-equal share with I in Al₂I⁻ (for which the natural and Mulliken charges are almost identical). This near-equally shared negative charge does not fit the relative EA values, since that for I is at least twice that for Al₂ (predicted, 1.2 eV; experimental, 1.5 eV²). The reason is therefore largely the positive-ionic character of the Al₂ moiety in Al₂I (\approx Al₂^{+0.5}I^{-0.5} in terms of the natural charges) attracting

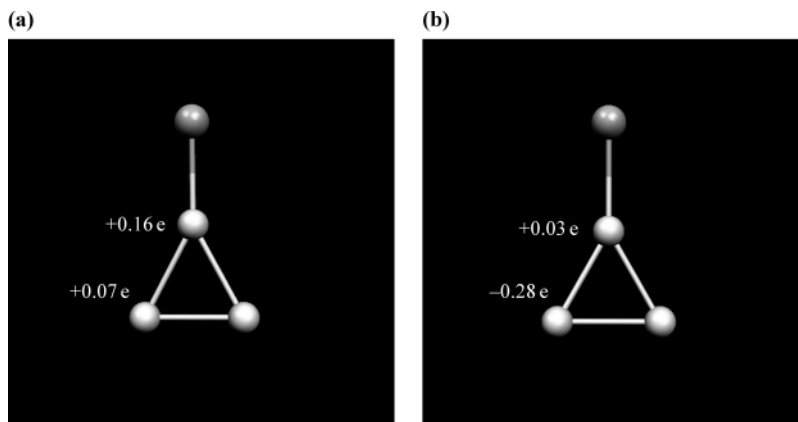


Figure 2. Optimized geometries and atomic natural charges of (a) Al_3I and (b) Al_3I^- .

the additional electron. Similar to the lithium species, the additional electron is localized almost entirely on the metal moiety, with the Mulliken charges showing a weaker localization. In particular, this is consistent with the relatively low EA values of AlI (0.5 eV) and Al_2I (1.4 eV). Again, the model of section Li^{13}I predicts negative EA for I^{\ominus} .

Al_3I . The rate of the negative-charge accumulation on the metal moiety in Al_nI^- with increasing size (Table 4) suggests crossing the -0.5 e level (equal share with iodine) well before $n = 13$. The Al_3I cluster has therefore been studied next. Among its isomers, the most stable one is found to be a C_{2v} -symmetric, Y-shaped flat structure with I near the central atom of the isosceles-triangular Al_3 (Figure 2). The ground state is predicted to be singlet, with the I-nearest Al distance slightly shorter than in AlI (Table 2) and the Al–Al distances of 2×2.57 and 2.43 Å, slightly away (up and down) from the (equilateral-triangle) Al_3 value of 2.53 Å. The charge separation between the metal and halogen moieties continues to reduce from Al_2I to Al_3I (Table 4) due to increasing electronegativity of Al_n , and the Mulliken charges remain more than twice as small as the natural ones. This is reflected in the calculated binding energy of I to Al_3 being 10% smaller than for Al_2I (Table 2). The Al_3I dipole moment is calculated to be 2.1 D.

Addition of an electron preserves the general Y-shape of the system while somewhat alters the interatomic distances, slightly stretching that for I-nearest Al (Table 2) and recovering the Al_3 moiety to the almost-equilateral triangle with sides of 2.53 ± 0.02 Å. The binding energy of I^- to Al_3 is ≈ 1 eV smaller than for the neutral counterpart (Table 2), and larger than for Al_2I^- and AlI^- (1.24 eV), likely due to increasing polarizability of the metal moiety. Search for other possible isomers of Al_3I^- is beyond the scope of this work.

As anticipated, the negative charge on the Al_3 moiety in Al_3I^- does exceed that on I (Table 4), according to both Mulliken and natural charge distributions (which are close to one another). The Al_3 cluster thus demonstrates a full-scale super-halogen behavior within Al_3I , similar to Al_{13} within Al_{13}I . Unlike for Al_{13} , however, this cannot be associated with the higher electron affinity of the isolated metal cluster relative to I, as the EA value of Al_3 is calculated to be 1.6 eV (compared to 1.9 eV experimental¹⁶), significantly lower than the iodine value. The main reason is therefore the predominant attraction of the additional electron to the metal moiety (positively charged within Al_3I). This is, in particular, consistent with the EA of Al_3I calculated to be 2.1 eV, close to the value for Al_3 . The other reason, indeed related to a higher electronegativity of Al_3 relative to Al_2 , is the sufficiently low, < 0.5 e, positive charge on the metal moiety in Al_3I (to be canceled by the additional electron).

Hence, the full-scale super-halogen behavior of Al_3 in Al_3I is induced by highly electronegative I creating positive charge on the metal moiety and is also due to its increased EA.

In Al_3I , the Al atom nearest to I carries most of the positive charge (Mulliken, $+0.09$ e: natural, $+0.16$ e) and is almost neutralized in Al_3I^- , while the two atoms more remote from I accept most of the additional negative charge (Figure 2). This is similar for both Mulliken and natural-charge distributions, and is consistent with the simple picture of the charge–dipole interaction (the additional charge repelling from the negative I).

Al_{13}I . In order to complete the comparison with the Al-based species, the Al_{13}I cluster is considered as well. Its and Al_{13}I^- structures have been predicted earlier⁸ and are reproduced here at the uniform level of theory applied throughout this work. The optimized geometries are shown in Figure 3 and parameterized in Table 2, and the charges are given in Table 4.

In Al_{13}I , the charge separation between the metal and halogen moieties is relatively small (less than in Al_3I), unlike in Li_{13}I , as a consequence of the higher electronegativity of Al_{13} compared to Li_{13} . In particular, this is consistent with the calculated binding energy of I to Al_{13} which is significantly less than for Li_{13}I as well as for Al_3I (Table 2). The decrease of the $\text{I}:\text{Al}_n$ binding with increasing n is opposite to the Li_nI case. The metal moiety in Al_{13}I is positively charged; therefore, in spite of EA of Al_{13} exceeding that of iodine, the latter is still more electronegative, apparently due to its significantly higher ionization energy. The dipole moment of Al_{13}I is, however, very small, ≈ 0.04 D, unlike for smaller clusters as well as for Li_{13}I .

As another result of the reduced charge separation, and again due to the dominant attraction of the additional electron to the positively charged metal moiety, the negative charge in Al_{13}I^- concentrates mainly on Al_{13} (Table 4), similar to the Al_3I^- case and different from Li_{13}I^- . The present results for the charges in Al_{13}I and Al_{13}I^- are very close to the data reported previously,^{8,14} and the Mulliken and natural charges are really close to one another in these systems. The trend of increasing negative charge on the metal moiety with its size continues from Al_3I^- to Al_{13}I^- .

Due to the EA value of Al_{13} exceeding that of I, the calculated binding energy of I^- to Al_{13} is larger than that of I to Al_{13}^- (Table 2), these two values being respectively somewhat higher and lower than the above $\text{I}:\text{Al}_{13}$ value. The increase of the binding energy between the halogen and (neutral) metal moieties from the neutral to the ionic system is opposite to its reduction for smaller clusters as well as for the lithium-based case. However, it is consistent with the binding energy variations with increasing cluster size, a decrease for the neutral and an increase

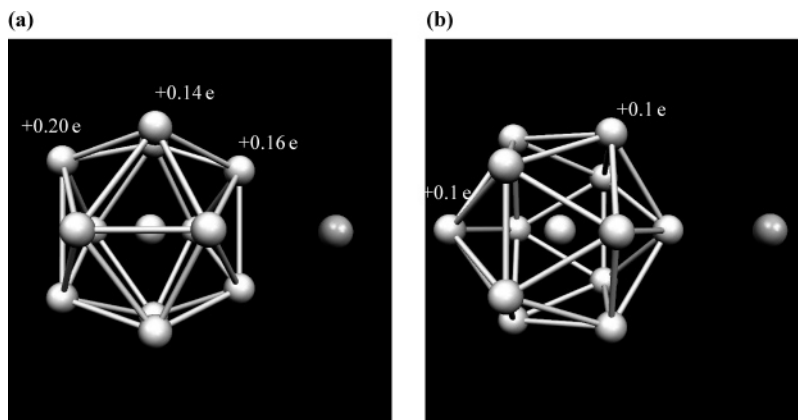


Figure 3. Optimized geometries and atomic natural charges of (a) Al_{13}I and (b) Al_{13}I^- .

for the ionic systems, so that the two sets intersect at some intermediate size between $n = 3$ and 13. A more precise determination of this intersection is beyond the scope of the present work.

Concerning other features of the predicted charge distribution, the Al atom in the center of the Al_{13} moiety in Al_{13}I carries a (natural) charge of -1.62 e, i.e., more than twice the value for Li_{13}I . The positive charge is distributed over the Al_{13} cluster periphery much more evenly (Figure 3a) than in the Li-based counterpart, the two Al atoms most remote from I being most positive. In isolated Al_{13} , the central-atom charge is -1.71 e. Unlike in the Li-based system, the corresponding Mulliken charges in Al_{13}I are quite reasonable, with $\text{Al}_{\text{center}}$ charged to $+0.41$ e and with the peripheral atoms slightly negative (up to -0.07 e). Essentially the same description (except for a more symmetric peripheral charge) applies to isolated Al_{13} , which is thus relatively weakly perturbed by I within Al_{13}I (true also for the natural charges).

In Al_{13}I^- , the central Al atom is slightly less negatively natural-charged (-1.44 e) than in Al_{13}I , in accord with its somewhat reduced charge (-1.51 e) in isolated Al_{13}^- relative to Al_{13} . This is different from the increased charge on $\text{Li}_{\text{center}}$ in Li_{13}I^- relative to Li_{13}I . Besides, the peripheral Al atoms in Al_{13}I^- remain slightly positive (Figure 3b). In terms of the Mulliken charges, however, $\text{Al}_{\text{center}}$ is more positive ($+0.63$ e), and the periphery is, accordingly, more negative in Al_{13}I^- than in Al_{13}I . By comparison, $\text{Al}_{\text{center}}$ in isolated Al_{13}^- is slightly less charged ($+0.56$ e). So again the influence of I is rather weak.

The negative-charge concentration on the opposite side of Al_3I^- from I (section AII and A2I) resembles the HOMO density in Al_{13}I^- concentrating on the Al atom most remote from iodine.⁸ Indeed, the additional electron in both Al_3I^- and Al_{13}I^- occupies HOMO, so the additional-charge distribution does describe the HOMO density. In Al_{13}I^- the additional negative-charge portion going to the Al atom on the opposite end of the cluster from I is the largest (-0.3 e), consistent with this atom being most positive ($+0.4$ e) in Al_{13}I (when frozen in the geometry of Al_{13}I^-) and with the repulsion of the additional electron from $\text{I}^{\delta-}$.

It should be noted once again that while the Mulliken and natural overall charges on Al_{13} are nearly identical in Al_{13}I as well as in Al_{13}I^- , they correspond to a positive or negative central Al atom in the Al_{13} moiety, respectively. The Mulliken version in this case appears to better fit the physical intuition, while suffering from the instability of the predicted charge values with respect to the level of accuracy. In particular, these values may vary appreciably for different DFT functionals, for

instance B3LYP relative to PBE (the former showing the positive charge on the central Al atom in Al_{13}I twice as large).

Conclusions

An ab initio investigation of Li_{13}I and Li_{13}I^- clusters has been performed at a DFT level of theory, and charge distributions analyzed at both the Mulliken and natural-charge levels. A comparison is made with smaller Li_nI species and Al-based analogues.

Optimized structures for both Li_{13}I and Li_{13}I^- show the iodine atom located at the hollow site between three Li atoms and the metal moiety generally preserving the icosahedral shape of the isolated Li_{13} cluster. Different spin states do, however, influence its geometry for the neutral system, varying from slightly elongated (in the direction of the I atom) for the ground triplet state to significantly compressed (by $\approx 10\%$) for the singlet state, with the dipole moment remaining unchanged. The ionic system shows only a weak perturbation of the metal moiety shape.

The Mulliken and natural charge distributions in Li_{13}I^- (as well as $\text{Li}_{13}^{\delta-}$) exhibit excessively positive and (unexpectedly) negative central Li atom, respectively, and oppositely charged periphery of the Li_{13} moiety which is overall positive in both cases. The natural charges on the lithium and iodine moieties are significantly larger (in absolute value). Both methods agree that in Li_{13}I^- the additional electron is localized predominantly on the metal moiety which is positively charged in the neutral system. This is consistent with the anticipated charge–dipole interaction. The same feature is present in smaller species, LiI and Li_2I . The alkali-metal components thus exhibit a super-halogen behavior in terms of winning the additional electron from the halogen atom in Li_nI^- , even though isolated Li_n are no super-halogens with low electron affinities.

A simple model interpretation is developed in terms of the metal and halogen moieties carrying charges within the system (i.e., $\text{Li}_{13}\text{I} = \text{Li}_{13}^{\delta+}\text{I}^{\delta-}$) and therefore having effective electron affinities (EA) very different from those for the isolated (neutral) components. Because these charges are due to the higher electronegativity of iodine, the super-halogen behavior of the metal moiety is induced by the halogen atom.

For a small enough partial charge (δ value) in the neutral system the additional electron (in the ionic system) still localized mainly on the metal moiety can make it more negative than iodine. This happens in Li_{13}I and even Li_2I according to the Mulliken charges but does not with the natural charges (corresponding to larger δ).

Comparison with the aluminum-based counterparts confirms the above considerations. The natural charges are smaller in

Al_nI than in Li_nI due to higher EA of Al_n , and decrease with increasing n , so the metal moiety in Al_nI^- accumulates negative charge more quickly with cluster size, exceeding the equal share with iodine at $n = 3$. The Mulliken charges are close to the natural charges in the Al_nI^- clusters. The Al_3 moiety thus exhibits a full-scale super-halogen behavior within Al_3I and is more negative than I in Al_3I^- , even though EA of isolated Al_3 is considerably smaller than that of isolated I.

A more metal-concentrated distribution of the negative charge in $Al_{13}I^-$ has been predicted previously⁸ and associated with EA of isolated Al_{13} exceeding that of isolated I (hence making the metal cluster a real super-halogen). Present results indicate that this is also due to the positive Al_{13} moiety in neutral $Al_{13}I$, hence due to the presence of I.

The observed trends suggest that Al_n ($n > 3$) moieties in Al_nI^- can be expected to behave like Al_3 and to be more negative than iodine even though their EA are smaller.²

The discussed phenomena can be used in analysis of other aluminum-halide clusters such as $Al_{13}X^{(-)}$ ($X = Br, Cl, F$) showing an increasing additional-electron loss by the metal moiety to the increasingly electronegative halogen moiety.¹⁷

Similar induced electron affinities and associated charge distributions are likely to be found in other cluster systems with components of different electronegativities. One example is $Al_{13}H^-$, with the extra negative charge carried entirely by the metal moiety, apparently due to the negatively charged H atom in $Al_{13}H$ ¹⁸ (similar to the $Al_{13}I^{(-)}$ case).

Knowledge of these properties is important for constructing materials from such systems as building blocks, in particular for a proper choice of counter ions in ionic crystals. The fusion of the metal clusters within a material could be prevented (besides their Coulomb repulsion) by appropriate spacers, such as ligands or maybe sufficiently large counter ions (perhaps other clusters).

Note Added in Proof. After this paper was submitted, new results were published by Y.-K. Han and J. Jung for the $Al_{14}I^-$ cluster (*J. Chem. Phys.* **2006**, *125*, 084101). They predict a charge of $-0.70e$ on the aluminum moiety (very close to our value for $Al_{13}I^-$), even though EA(Al_{14}) is much lower than EA(I). This thus further supports our predictions. Han and Jung

also state that the jellium model may be inappropriate for such clusters. This is supported by our finding of the triplet rather than singlet ground state for $Li_{13}I$, which has 20 valence electrons from its atoms.

Acknowledgment. The authors acknowledge the technical assistance of Dr. Thomas Hu regarding the UOIT/Science computing facilities administration. A part of the calculations has been performed using the computing facilities in the University of Toronto/Department of Chemistry. H.L. is grateful to the UOIT for the Undergraduate Summer Research Award.

References and Notes

- (1) Alonso, J. A. *Chem. Rev.* **2000**, *100*, 637.
- (2) Li, X.; Wu, H.; Wang, X.; Wang, L. *Phys. Rev. Lett.* **1998**, *81*, 1909.
- (3) Taylor, K. J.; Pettiette-Hall, C. L.; Cheshnovsky, O.; Smalley, R. E. *J. Chem. Phys.* **1992**, *96*, 3319.
- (4) Zhai H.-J.; Li, J.; Wang, L.-S. *J. Chem. Phys.* **2004**, *121*, 8369.
- (5) Gutsev, G. L.; Boldyrev, A. I. *Chem. Phys.* **1981**, *56*, 277.
- (6) Wang, X.-B.; Ding, C.-F.; Wang, L. S.; Boldyrev, A. I.; Simons, J. *J. Chem. Phys.* **1999**, *110*, 4763.
- (7) Elliott, B. M.; Koyle, E.; Boldyrev, A. I.; Wang, X.-B.; Wang, L.-S. *J. Phys. Chem. A* **2005**, *109*, 11560.
- (8) Bergeron, D. E.; Castleman, A. W., Jr.; Morisato, T.; Khanna, S. N. *Science* **2004**, *304*, 84; *J. Chem. Phys.* **2004**, *121*, 10456.
- (9) Aprà, E.; Windus, T. L.; Straatsma, T. P.; Bylaska, E. J.; de Jong, W.; et al. *NWChem A Computational Chemistry Package for Parallel Computers*, Version 4.7; Pacific Northwest National Laboratory: Richland, WA, 2005. <http://www.emsl.pnl.gov/docs/nwchem/>.
- (10) Flükiger P.; Lüthi, H. P.; Portmann, S.; Weber, J. *MOLEKEL 4.0*; Swiss Center for Scientific Computing: Manno, Switzerland, 2000. <http://www.cscs.ch/molekel/>.
- (11) Schultz, N. E.; Staszewska, G.; Staszewski, P.; Truhlar, D. G. *J. Phys. Chem. B* **2004**, *108*, 4850.
- (12) *NIST Chemistry WebBook*; NIST Standard Reference Database No. 69, June, 2005 Release. <http://webbook.nist.gov/chemistry/>.
- (13) Fournier, R.; Cheng, J. B. Y.; Wong, A. *J. Chem. Phys.* **2003**, *119*, 9444.
- (14) Han Y.-K.; Jung, J. *J. Chem. Phys.* **2004**, *121*, 8500.
- (15) Autschbach, J.; Hess, B. A.; Johansson, M. P.; Neugebauer, J.; Patzschke, M.; Pyykkö, P.; Reiher, M.; Sundholm, D. *Phys. Chem. Chem. Phys.* **2004**, *6*, 11.
- (16) Wu, H.; Li, X.; Wang, X.-B.; Ding, C.-F.; Wang, L.-S. *J. Chem. Phys.* **1998**, *109*, 449.
- (17) Jung, J.; Kim, J. C.; Han, Y.-K. *Phys. Rev. B* **2005**, *72*, 155439.
- (18) Han, Y.-K.; Jung, J.; Kim, J. C. *J. Chem. Phys.* **2005**, *122*, 124319.